The Extended-Range Comprehensive Atmospheric Optics Sensing (ERCAOS) Campaign: Overview

Mikhail Vorontsov[1,2], Ernst Polnau[1], Thomas Weyrauch[1] & Victor Kulikov[1]

[1] Intelligent Optics Laboratory,
Department of Electro-Optics and Photonics,
University of Dayton

[2] II-VI-Optonicus Inc

Communications and Observations through Atmospheric Turbulence (COAT): Characterization and Mitigation

- Dates/Location: Dec. 2nd & 3rd 2019 @ ONERA (Paris south-suburb)

Supported by AFOSR MURI contract #FA9550-12-1-0449
"Wave Optics of Deep Atmospheric Turbulence: From Underlying Physics towards Predictive Modeling, Mitigation and Exploration"

University of Dayton

Outline

- Objectives, Team, Propagation Path
- Instrumentation
- Pupil-plane intensity scintillations (0.53 μm and 1.06 μm)
- Beam footprint and refractivity estimation with 3-wavelength polychromatic laser beacon
- Power-in-the-bucket fluctuations & giant spikes observation
- Summary

Propagation Path & Experimental Settings

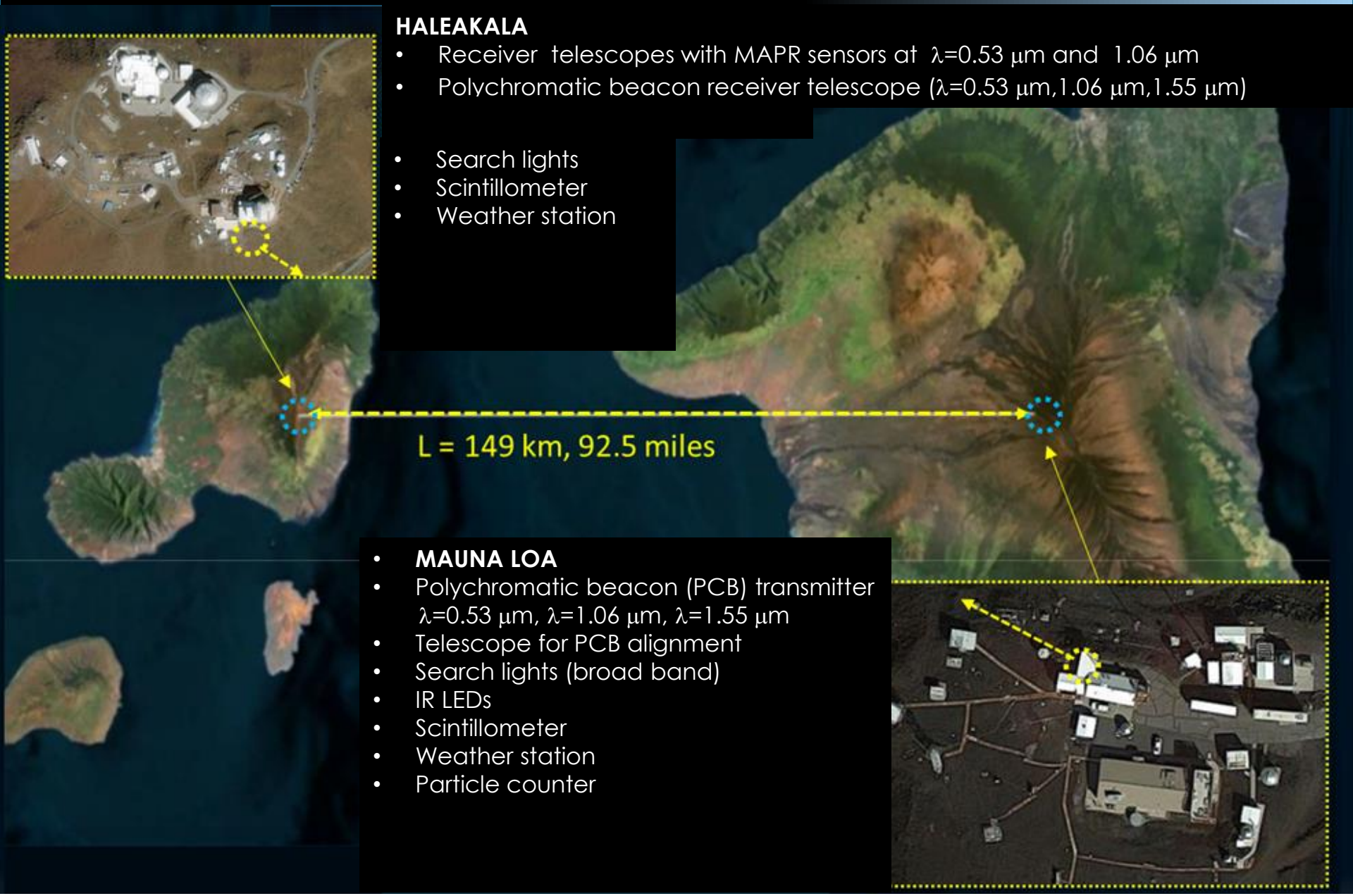

HALEAKALA

- Receiver telescopes with MAPR sensors at λ=0.53 μm and 1.06 μm
- Polychromatic beacon receiver telescope (λ=0.53 μm,1.06 μm,1.55 μm)
- Search lights
- Scintillometer
- Weather station

- **MAUNA LOA**
- Polychromatic beacon (PCB) transmitter λ=0.53 μm, λ=1.06 μm, λ=1.55 μm
- Telescope for PCB alignment
- Search lights (broad band)
- IR LEDs
- Scintillometer
- Weather station
- Particle counter

Propagation Geometry

Experiments were performed over the propagation path of length L=149.2 km between the laser beacon platform located on the Mauna Loa mountain (Hawaii island) at elevation h_{ML} = 3397 m (11,140 ft), and the 30.5-cm receiver telescope on the top of the Haleakala mountain (Maui island) at elevation h_H = 3058 m. Due to the Earth's curvature, the minimum height along the propagation path h_{min} = 2775 m corresponds to the distance 60 km from the Haleakala site.

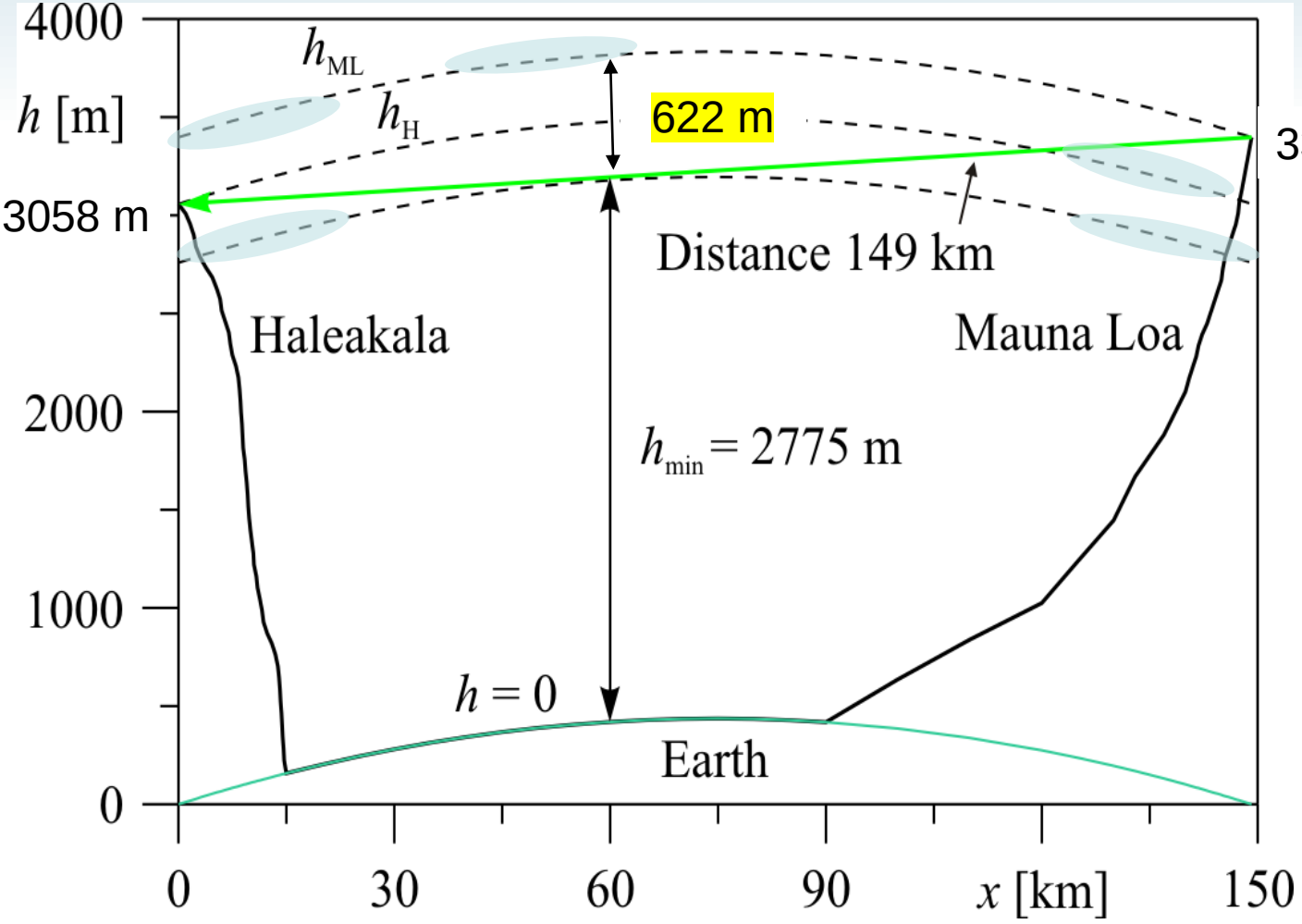

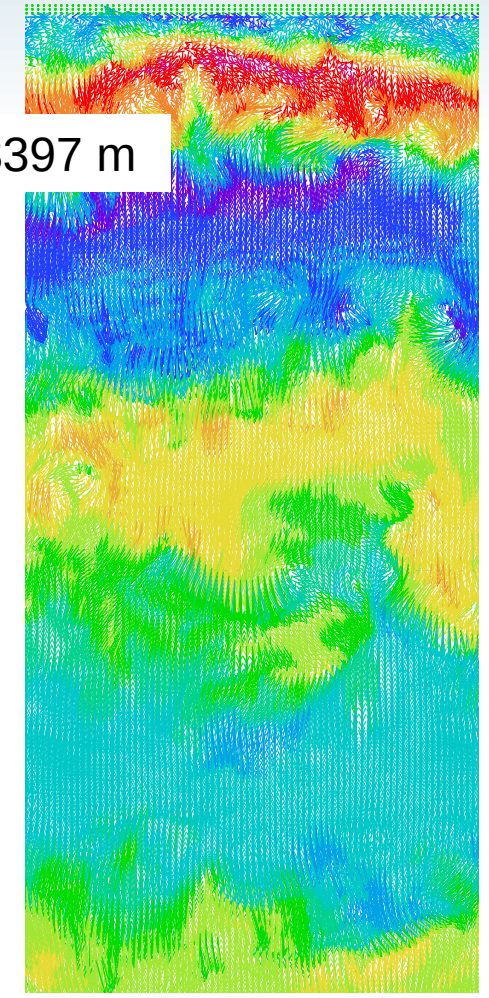

Haleakala Site

Optical Systems at Haleakala Site

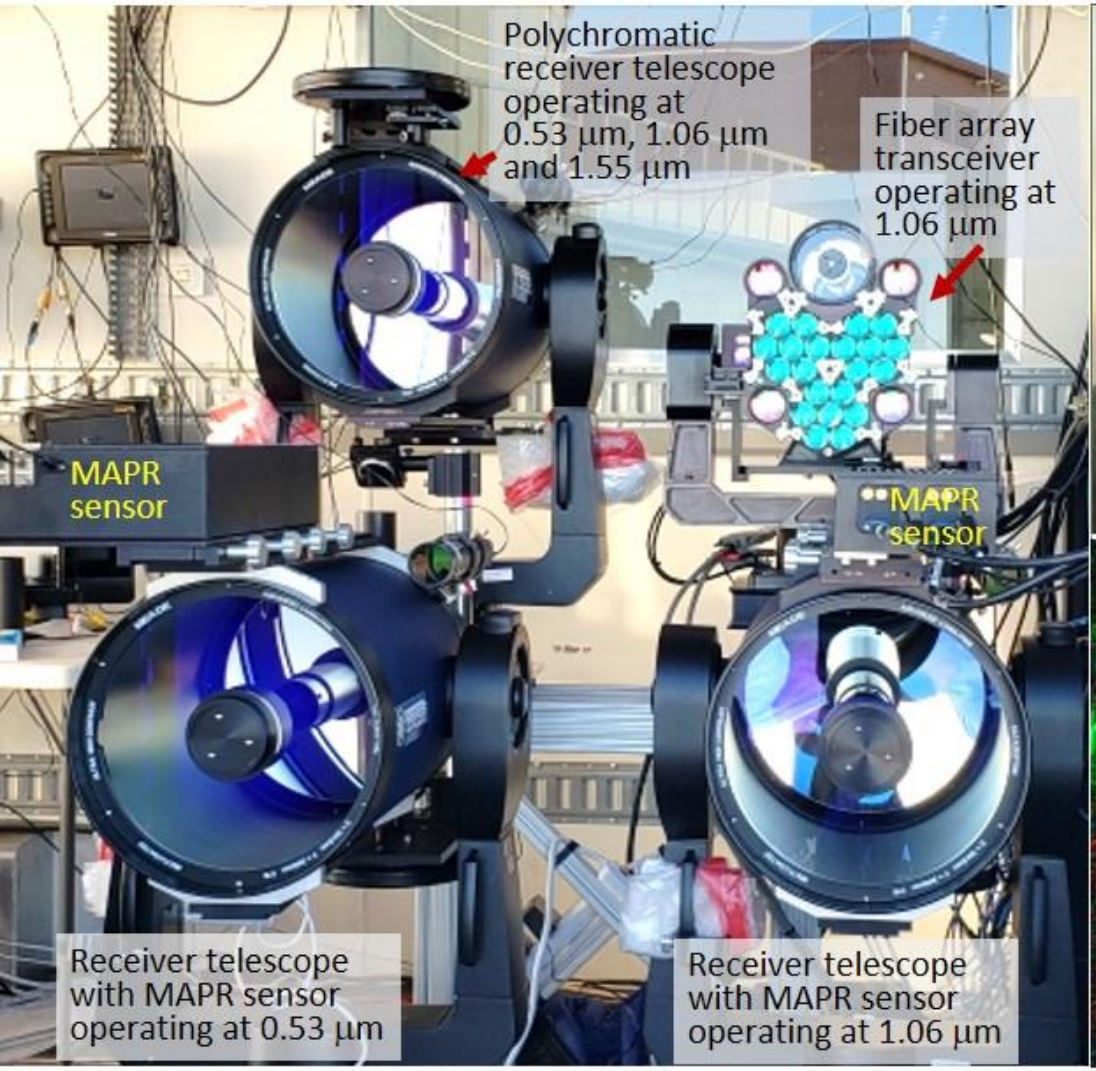

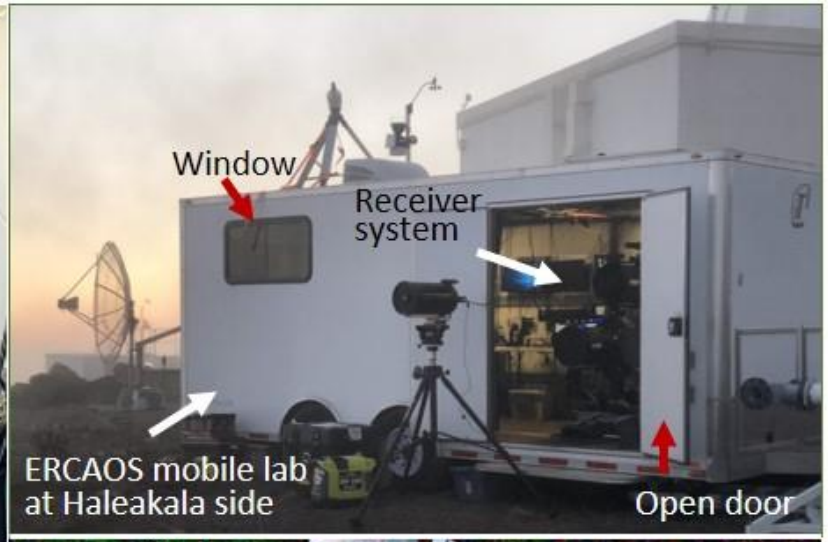

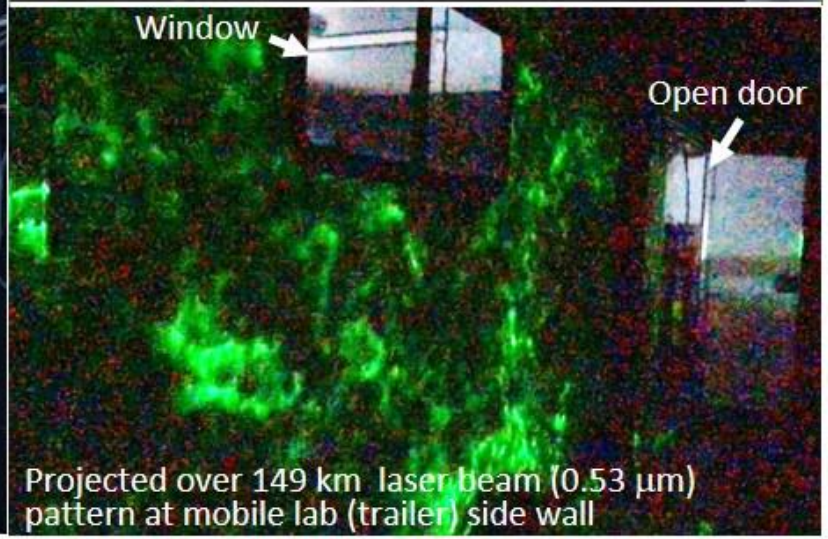

ERCAOS experimental setting at the Haleakala site: receiver system inside the mobile lab (left), view of the mobile lab at Haleakala site during experiments (top, right), and a characteristic image of laser beam seen at the mobile lab side wall (bottom right).

Optical Systems at Haleakala Site: Polychromatic Receiver System

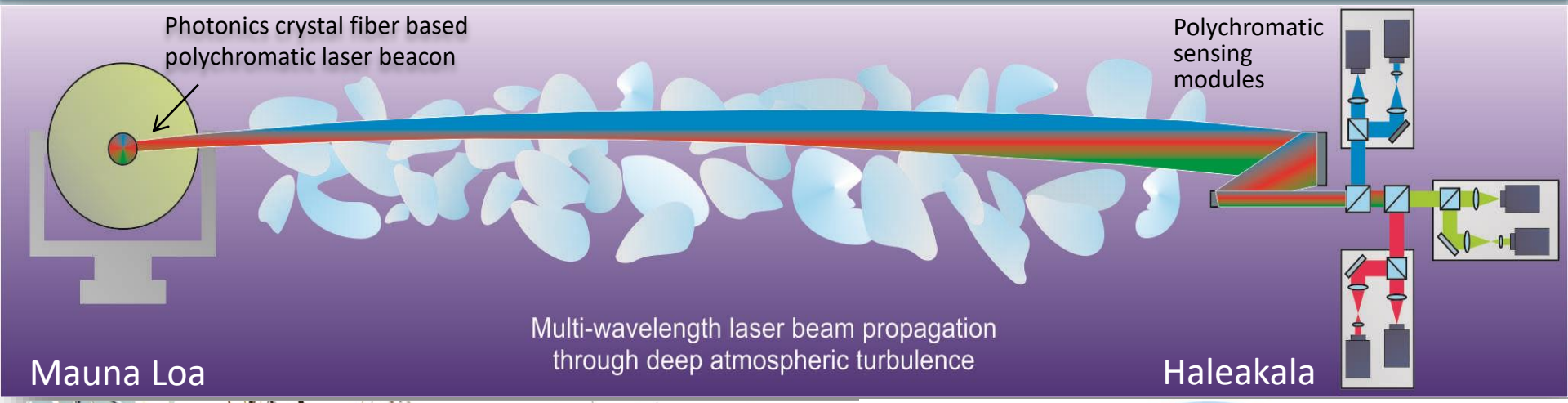

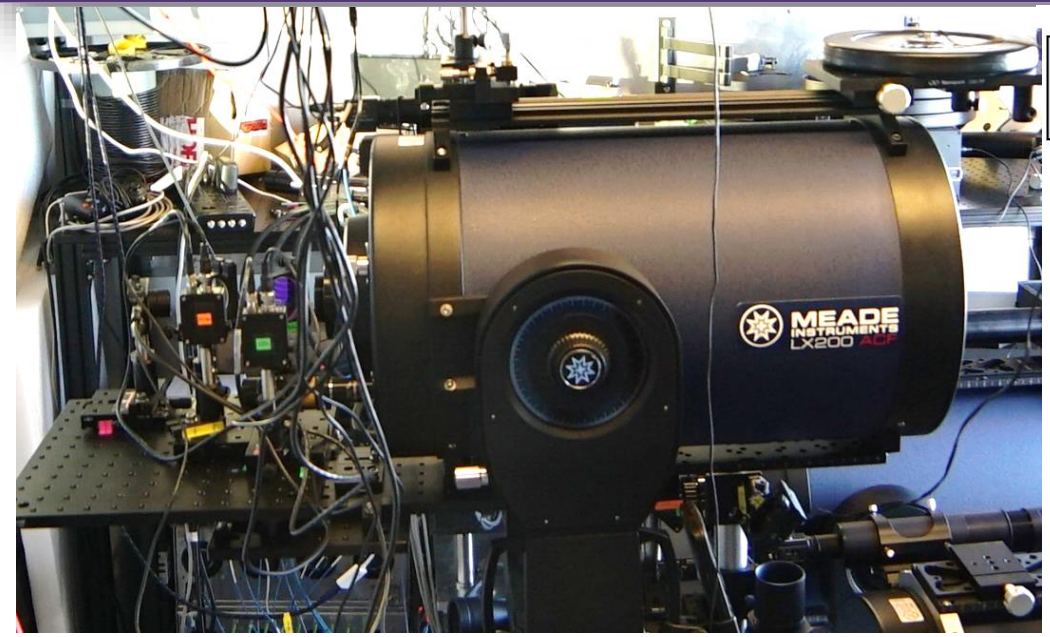

Polychromatic receiver is power-in-the-bucket (PIB) sensor based on 30.48 cm Meade telescope and three optical channels with single-pixel photo detectors

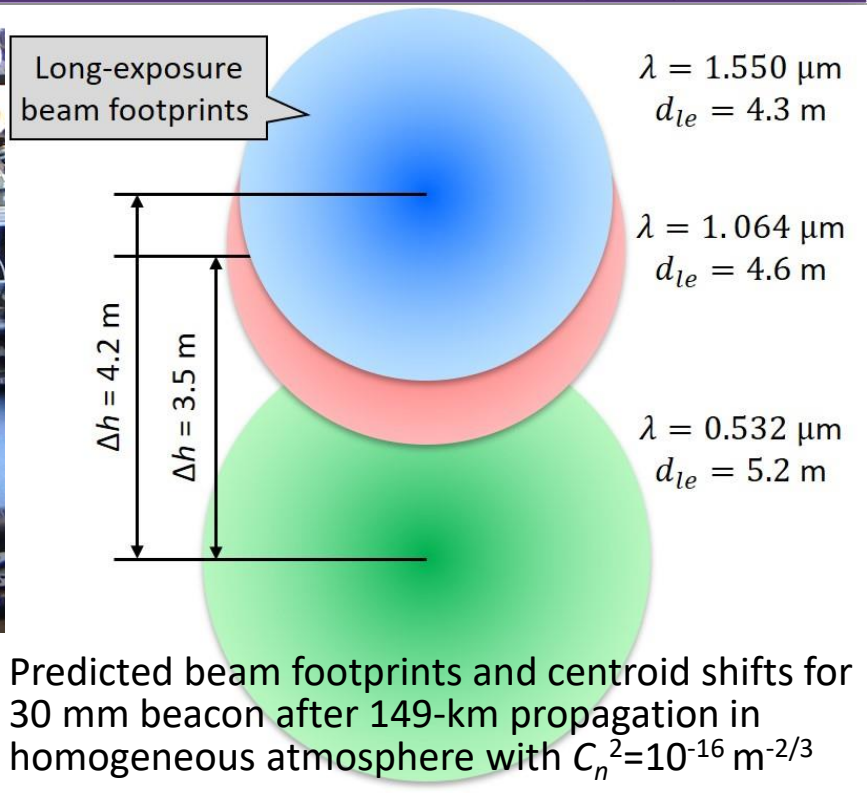

Predicted beam footprints and centroid shifts for 30 mm beacon after 149-km propagation in homogeneous atmosphere with $C_n^2=10^{-16}$ m$^{-2/3}$

Mauna Loa Site: Polychromatic Beacon

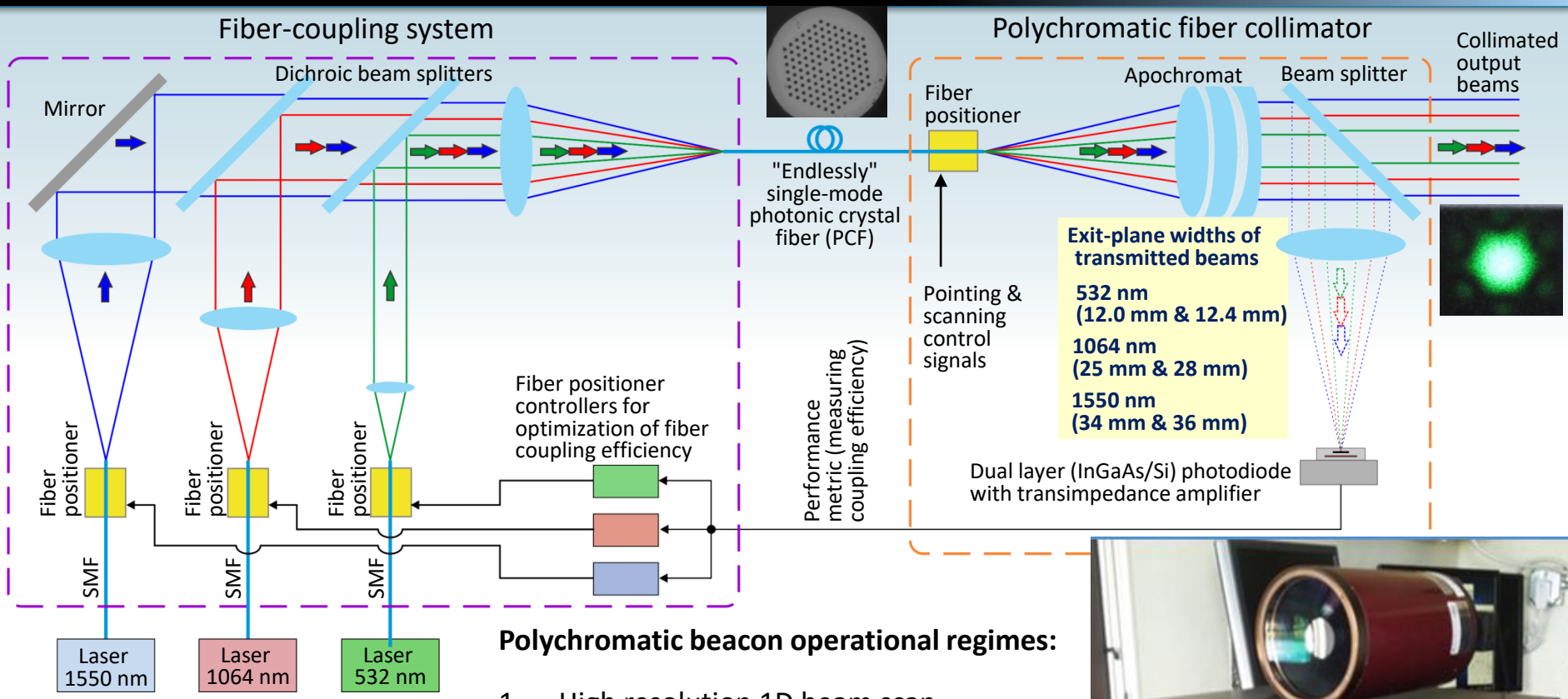

Beacon scanning area at 149 km

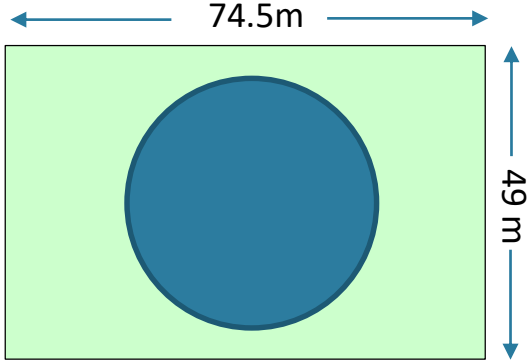

Polychromatic beacon operational regimes:

1. High resolution 1D beam scan (vertical or horizontal) with continuous measurements of received power inside 30.5 cm bucket for each wavelength
2. High resolution 2D beam scan with continuous measurements of received power inside 30.5 cm bucket for each wavelength
3. low-resolution 1D beam scan (vertical or horizontal) with continuous measurements of received power inside 30.5 cm bucket for each wavelength

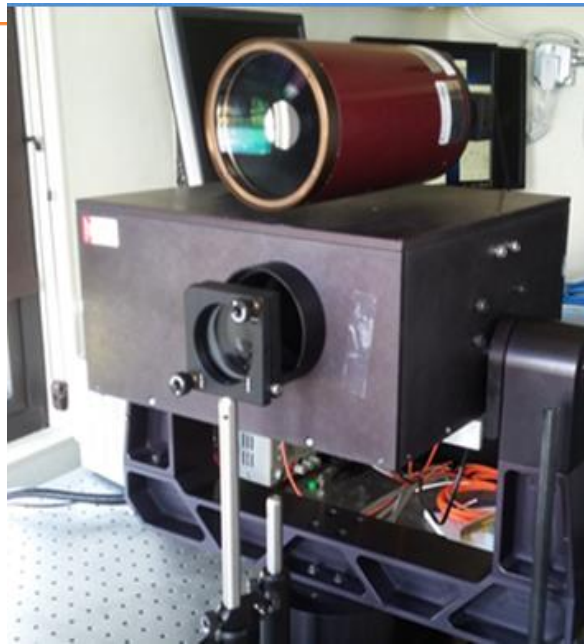

Mauna Loa Site: Polychromatic Beam Propagation

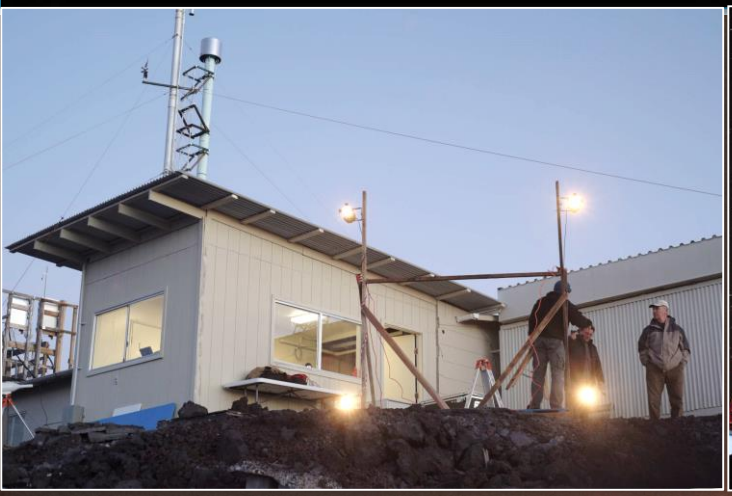

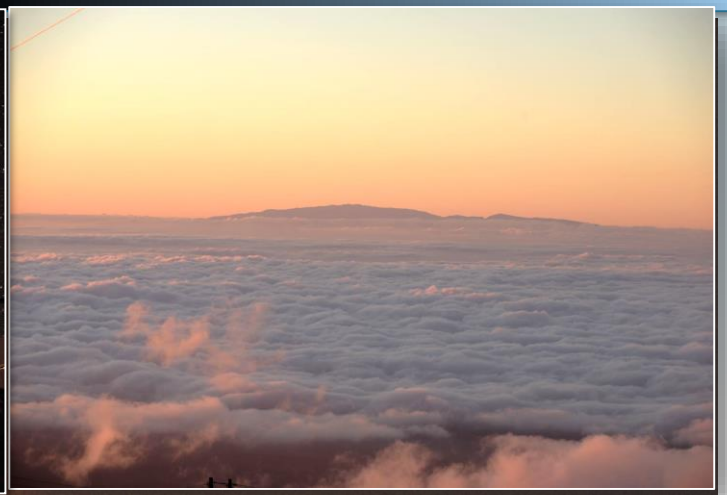

Video of Intensity Scintillations at Haleakala Site

April 6, 2019

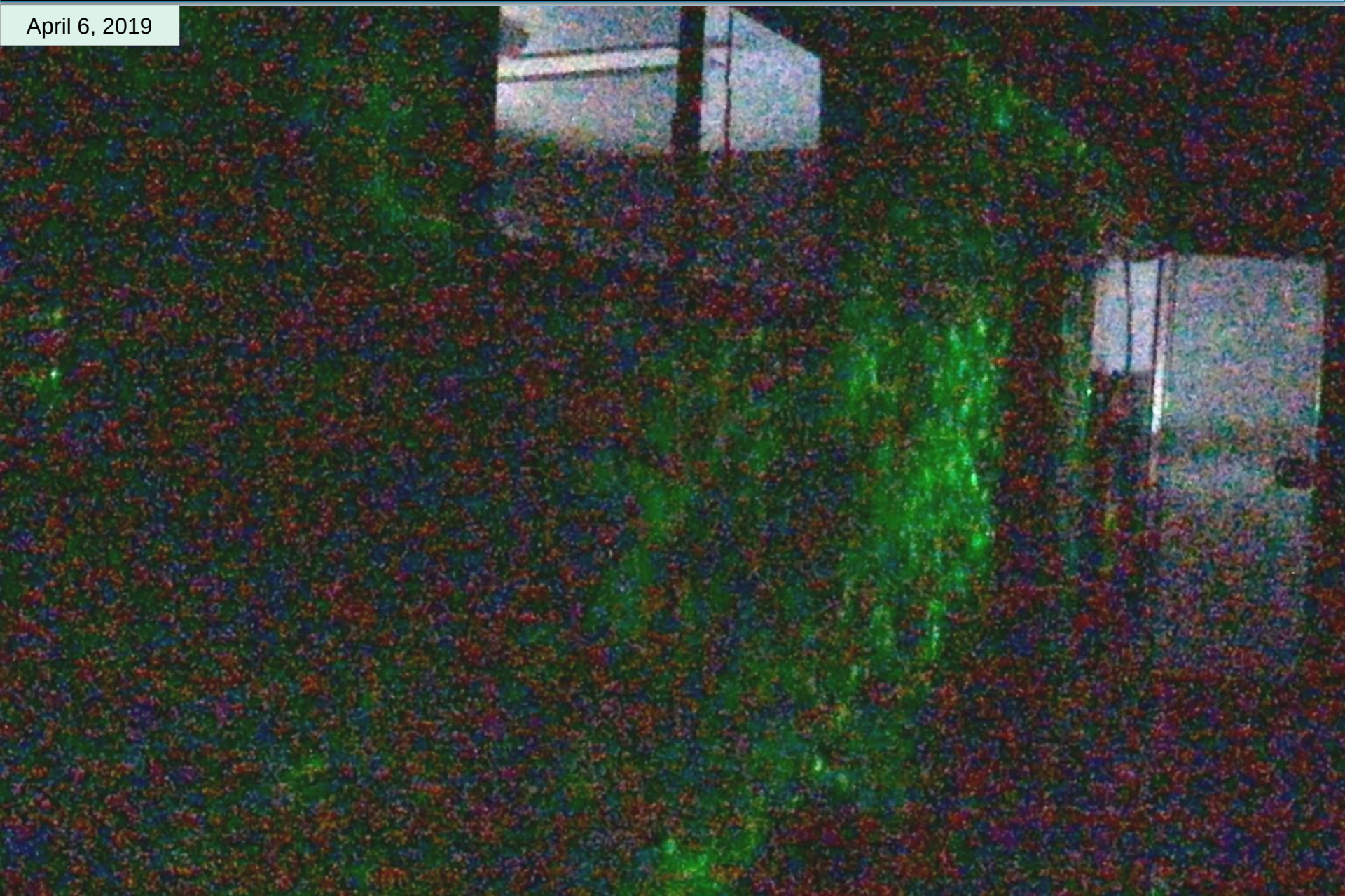

Video of Intensity Scintillations at Haleakala Site

April 9, 2019

Video of Intensity Scintillations at Haleakala Site

April 15, 2019

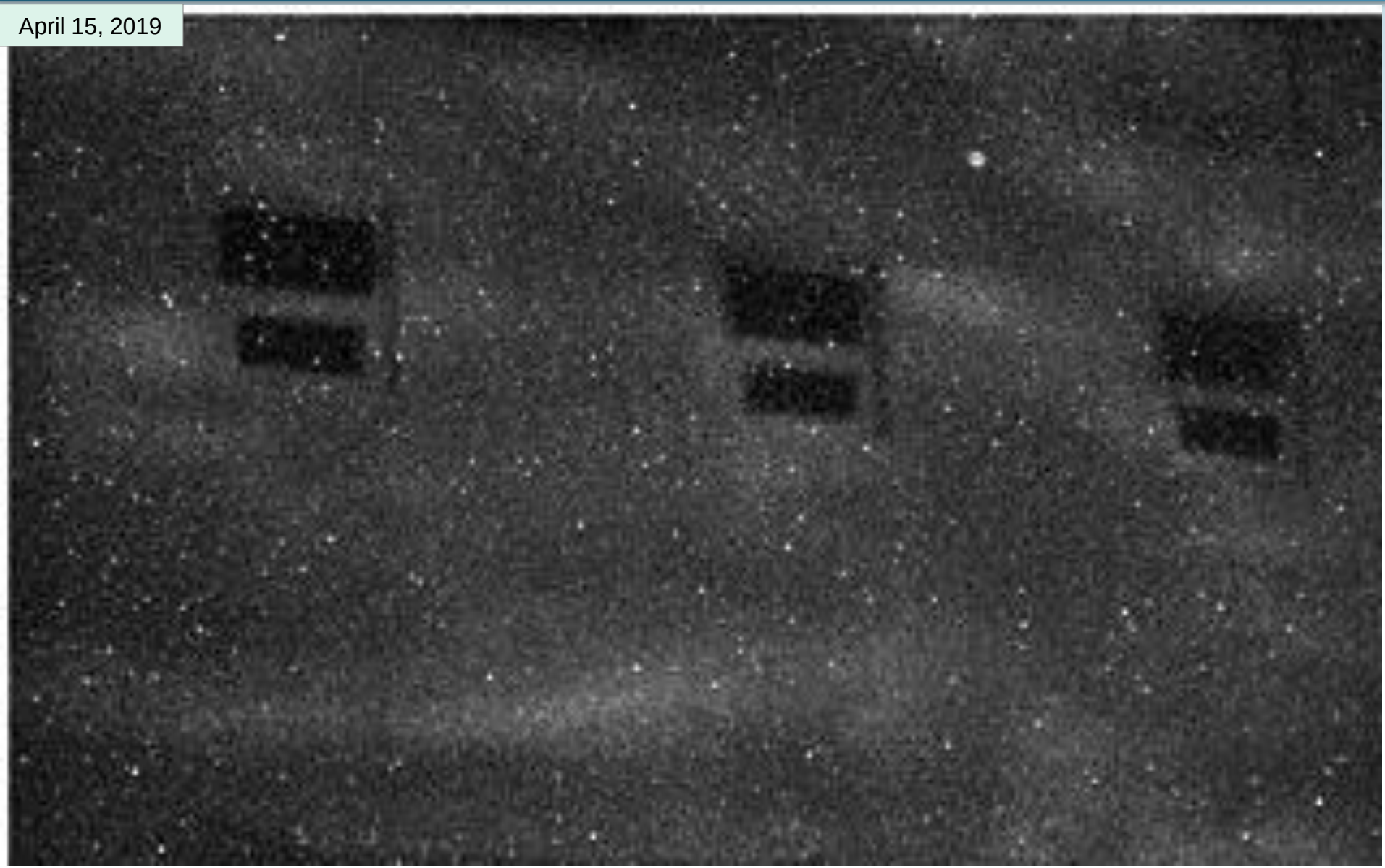

Samples of Pupil-Plane Short-Exposure Intensity Distributions (April 4)

λ=532 nm; 211 frames/sec

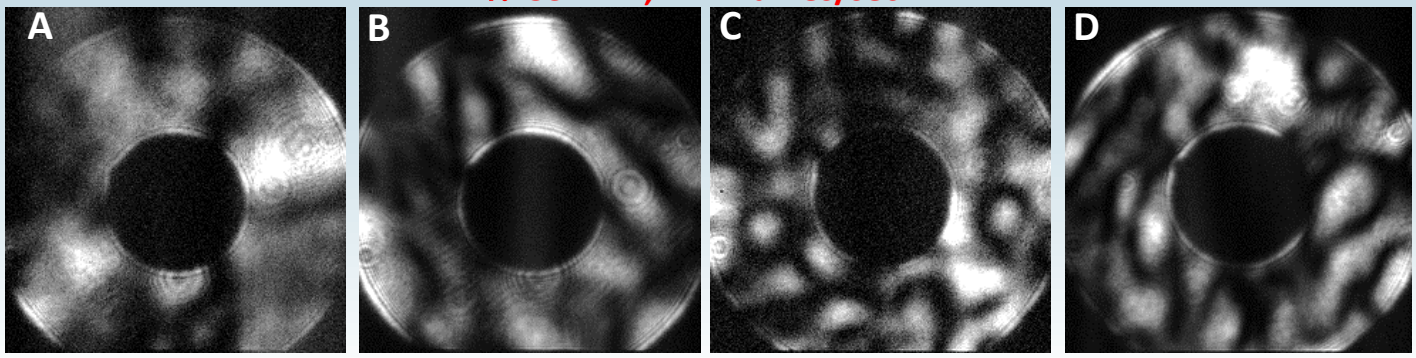

A: Integration time $6 \cdot 10^{-6}$ sec
recording at 20:33:03
frame #5784 at 20:33:30.38
B: Integration time $2.3 \cdot 10^{-5}$ sec
recording at 20:59:31.42
frame #6074 at 21:00:00.21
C: Integration time $2.3 \cdot 10^{-5}$ sec
recording at 22:09:01.67
frame #1766 at 22:09:10.04
D: Integration time $2.3 \cdot 10^{-5}$ sec
recording at 22:43:18.09
frame #1280 at 22:43:24.15

λ=1064 nm; 59 frames/sec

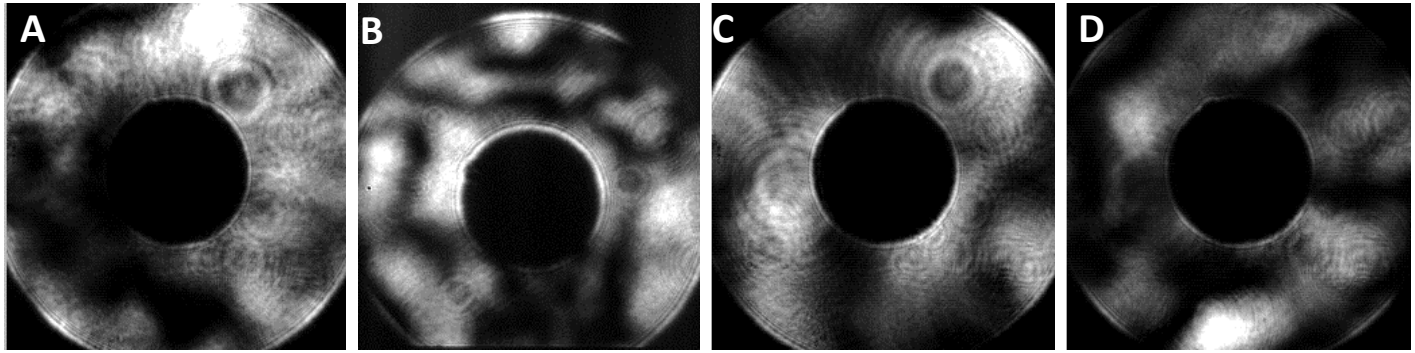

A: Integration time $1 \cdot 10^{-3}$ sec
recording at 20:33:37.51
frame #47 at 20:33:38.31
B: Integration time $1 \cdot 10^{-3}$ sec
recording at 21:00:05.92
frame #7 at 21:00:06.04
C: Integration time $1 \cdot 10^{-3}$ sec
recording at 22:09:36.20
frame #48222:09:44.37
D: Integration time $1 \cdot 10^{-3}$ sec
recording at 22:43:52.61
frame #383 at 22:43:59.10

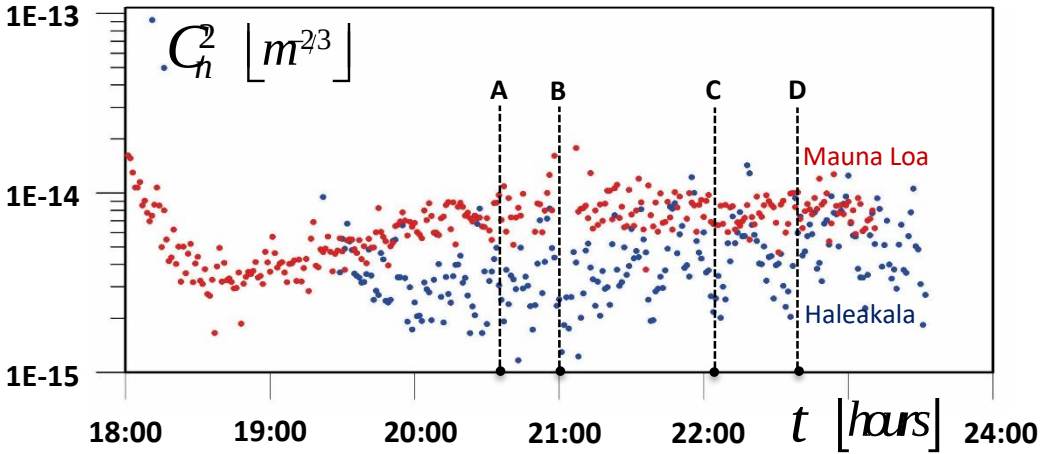

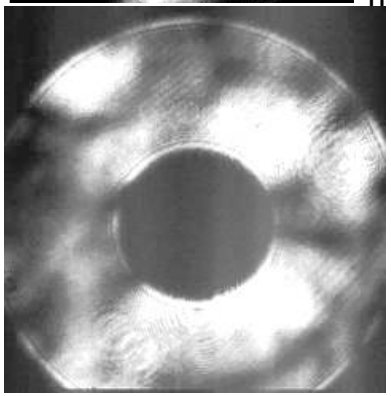

λ=532 nm

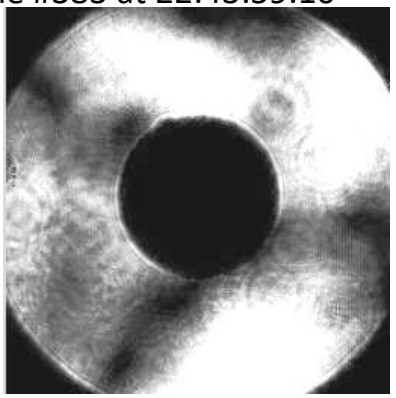

λ=1064 nm

Analysis of Video Sequences: Pupil Plane Scintillations (April 4)

Time-averaged variance of intensity non-homogeneity within receiver aperture ("spatial" fluctuations variance)

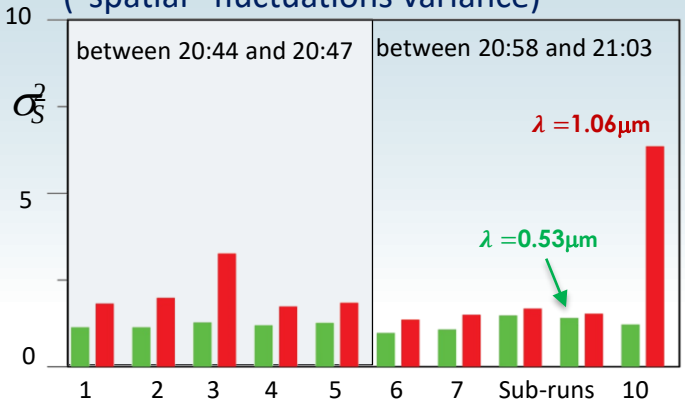

Intensity scintillations probability density function (PDF) for 30 sec recording (sub-run #8, 6125 frames)

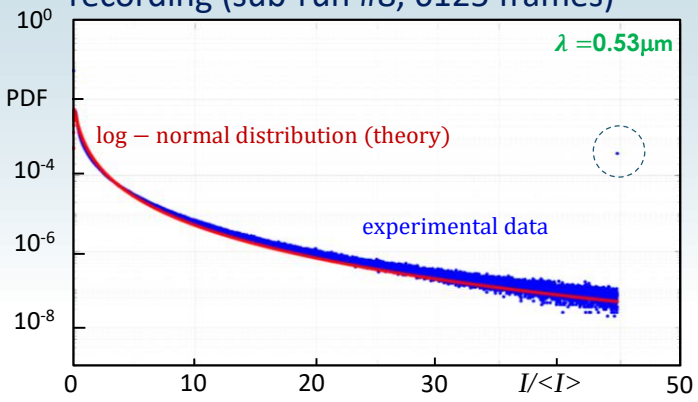

Aperture-averaged variance of intensity fluctuations for *n*-th frame

$$\sigma_S^2(n)=\left\langle\left[I_n(\mathbf{r}_m)-\bar{I}_n\right]^2\right\rangle_S\Big/\bar{I}_n^2$$

averaged intensity inside n[th] frame

Time/frame- averaged variance of intensity fluctuations within receiver aperture ("spatial" variance)

$$\sigma_S^2=\left\langle\sigma_S^2(n)\right\rangle_N$$

Aperture-averaged variance of intensity fluctuations ("temporal" fluctuations variance)

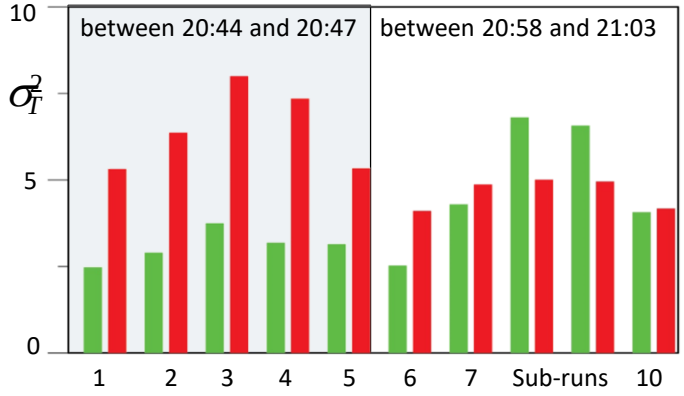

Comparison of temporal and spatial variances of intensity fluctuations

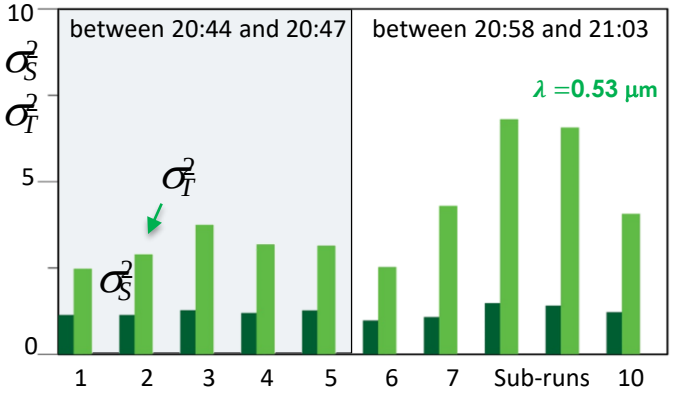

Variance of intensity fluctuations (1x1 mm pixel)

$$\sigma_N^2(\mathbf{r}_m)=\frac{\left\langle\left[I_n(\mathbf{r}_m)-\bar{I}_n(\mathbf{r}_m)\right]^2\right\rangle_N}{\bar{I}^2(\mathbf{r}_m)}$$

Averaged over aperture area variance of intensity fluctuations inside a pixel ("temporal" variance)

$$\sigma_T^2=\left\langle\sigma_N^2(\mathbf{r}_m)\right\rangle_{aperture}$$

Recording parameters

Number of frames for λ_1=0.53 μm	N=6050-6240 frames
Number of frames for λ_2=1.06 μm	N=1710-1770 frames
Duration of recording at both λ_1 and λ_2	30 sec

Experimental setup characteristic sizes

Aperture diameter	305 mm
Central obscuration diameter	102 mm
Pixel size	1mm x1 mm

Pupil Plane Scintillations (April 5)

λ=532 nm; 211 frames/sec

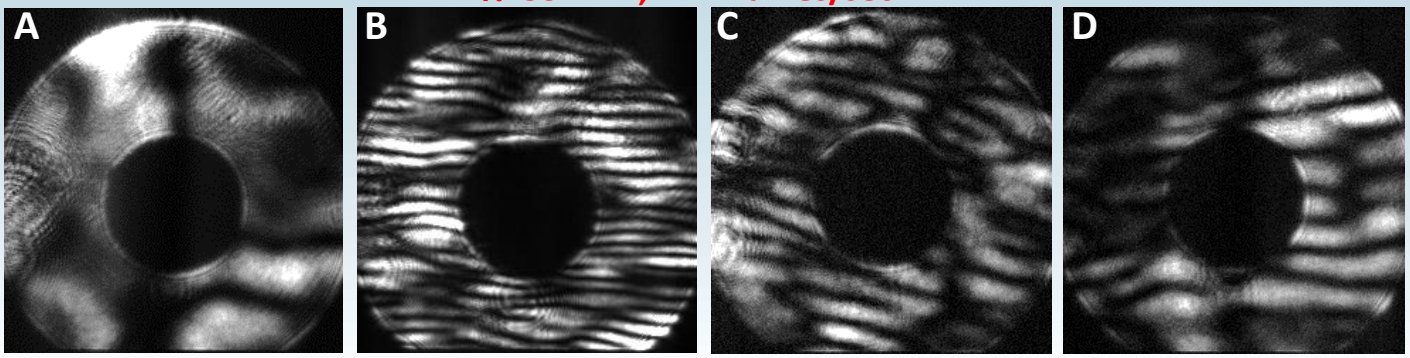

A: Integration time $2 \cdot 10^{-5}$ sec
recording at 19:48:16.01
frame #5 at 19:48:16.05
B: Integration time $2 \cdot 10^{-5}$ sec
recording at 20:56:56
frame #363 at 21:00:00.21
C: Integration time $2 \cdot 10^{-5}$ sec
recording at 22:18:23
frame #23 at 22:18:23.25
D: Integration time $2 \cdot 10^{-5}$ sec
recording at 22:28:28
frame #1280 at 22:28:35.77

λ=1064 nm; 59 frames/sec

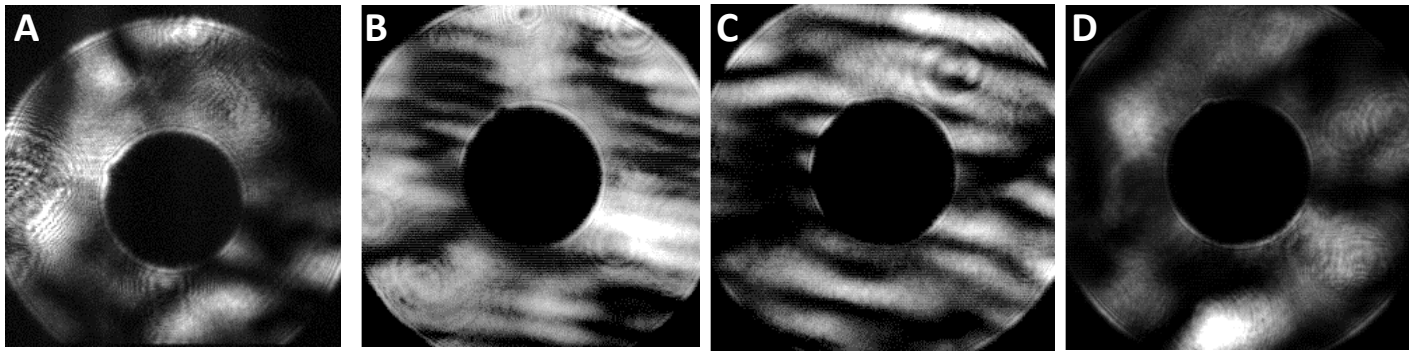

A: Integration time $1 \cdot 10^{-3}$ sec
recording at 19:48:16.01
frame #3 at 19:48:16.05
B: Integration time $1 \cdot 10^{-3}$ sec
recording at 21:00:05.92
frame #132 at 21:00:06.04
C: Integration time $1 \cdot 10^{-3}$ sec
recording at 22:18:57.45
frame #1321 at 22:19:19.84
D: Integration time $1 \cdot 10^{-3}$ sec
recording at 22:29:03.22
frame #474 at 22:29:11.26

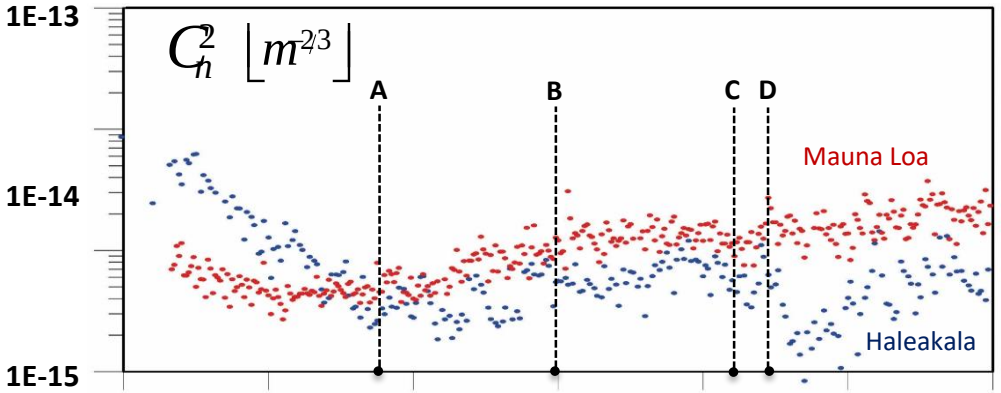

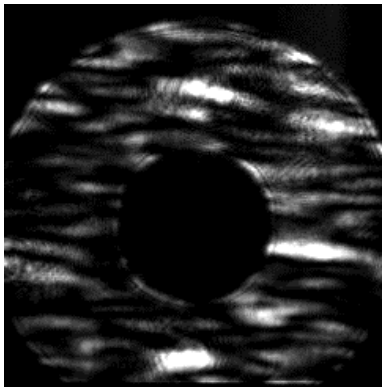

λ=532 nm

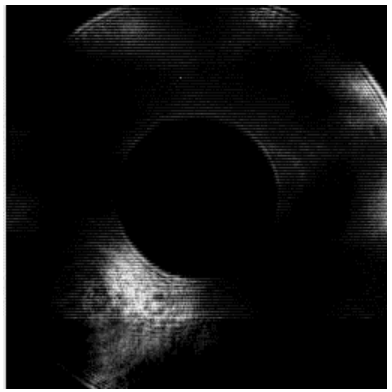

λ=1064 nm

Coherent Laser Beam Mirages (April 5)

Pupil (top) and focal (bottom) intensities λ=532 nm; 211 frames/sec

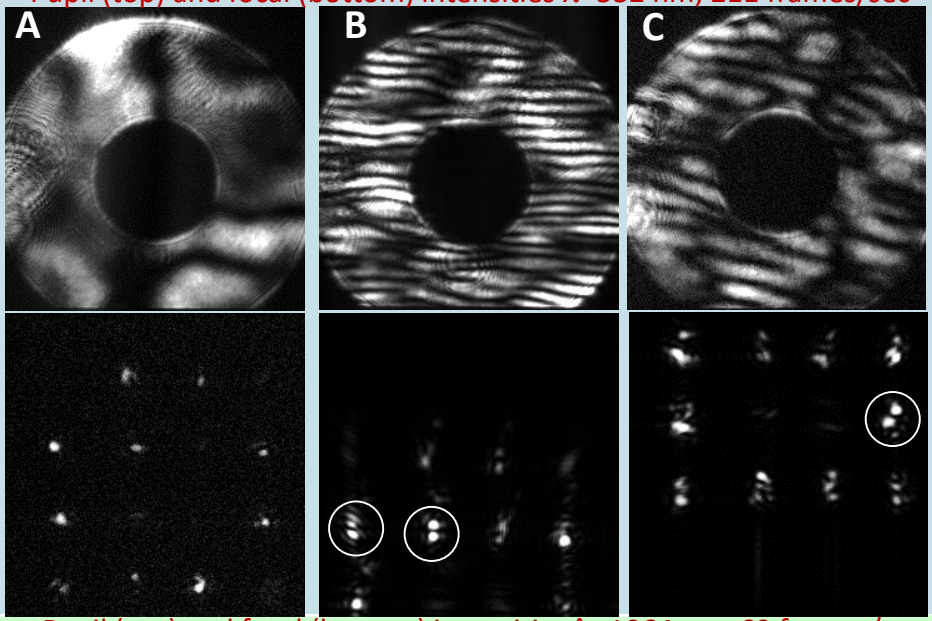

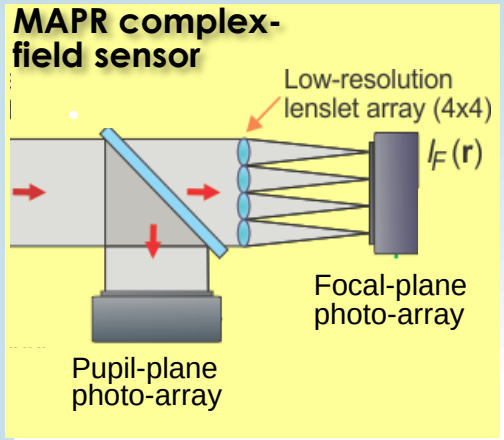

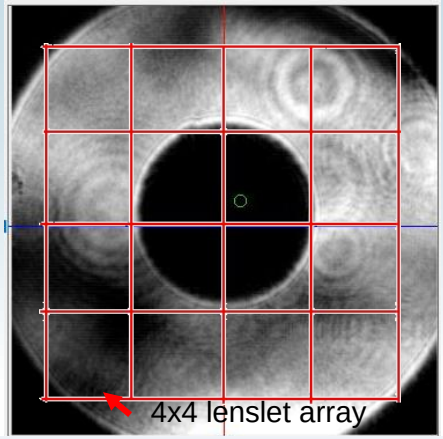

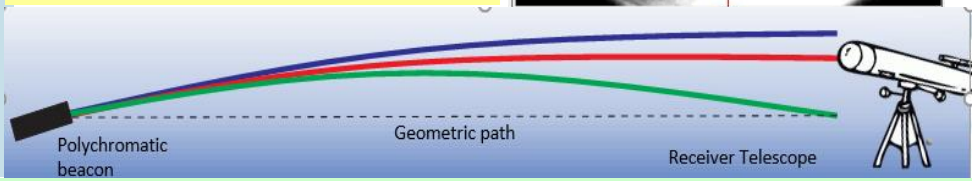

Pupil (top) and focal (bottom) intensities λ=1064 nm; 60 frames/sec

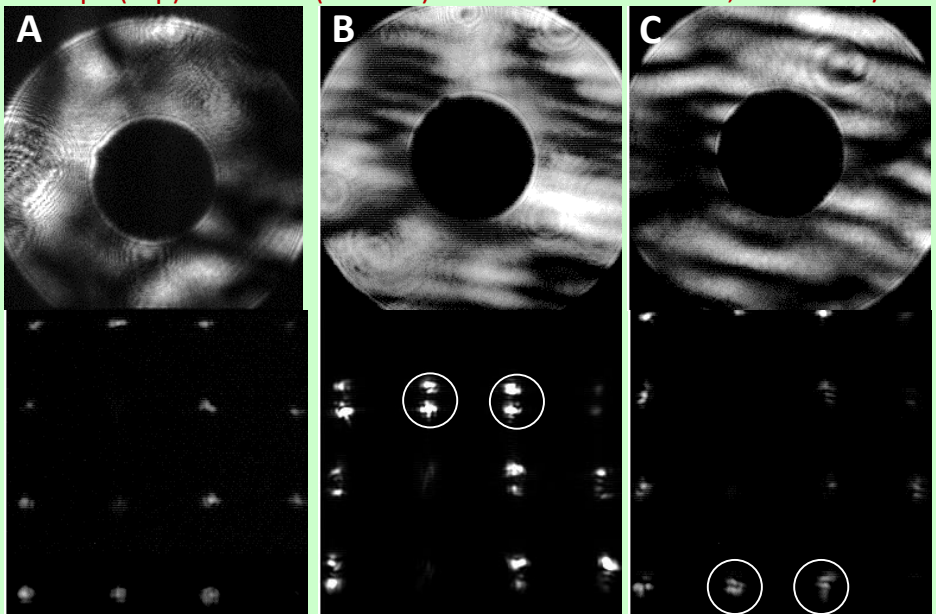

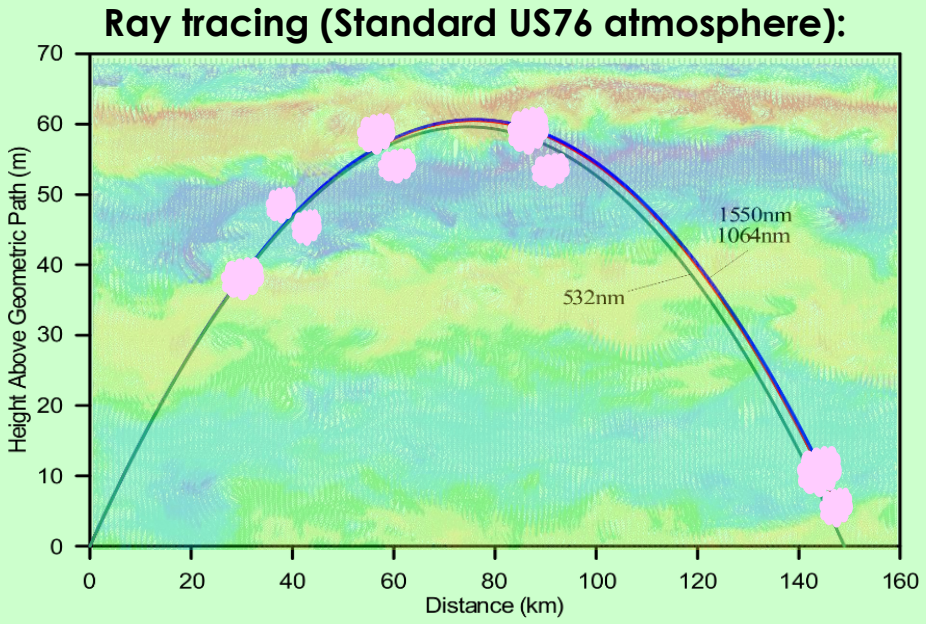

Analysis of Video Sequences: Pupil Plane Scintillations (April 5)

Time-averaged variance of intensity non-homogeneity within receiver aperture ("spatial" fluctuations variance)

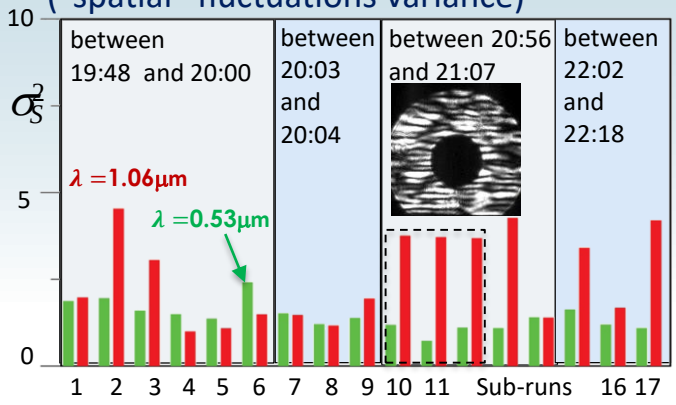

Intensity scintillations probability density function (PDF) for 30 sec recording (sub-run #1, 2921 frames)

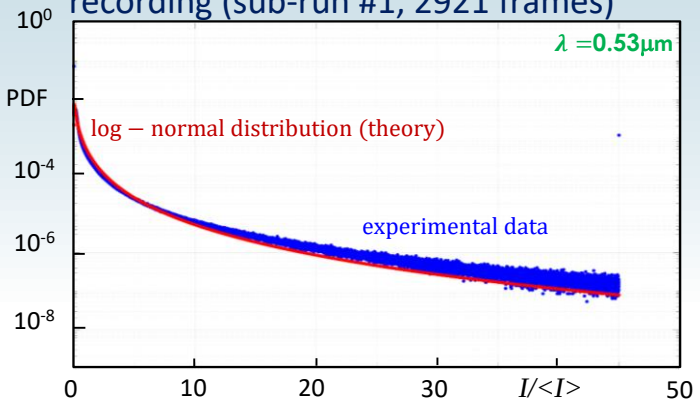

Aperture-averaged variance of intensity fluctuations for *n*-th frame

$$\sigma_S^2(n)=\left\langle\left[I_n(\mathbf{r}_m)-\bar{I}_n\right]^2\right\rangle_S\Big/\bar{I}_n^2$$

averaged intensity inside nth frame

Time/frame- averaged variance of intensity fluctuations within receiver aperture ("spatial" variance)

$$\sigma_S^2=\left\langle\sigma_S^2(n)\right\rangle_N$$

Aperture-averaged variance of intensity fluctuations ("temporal" fluctuations variance)

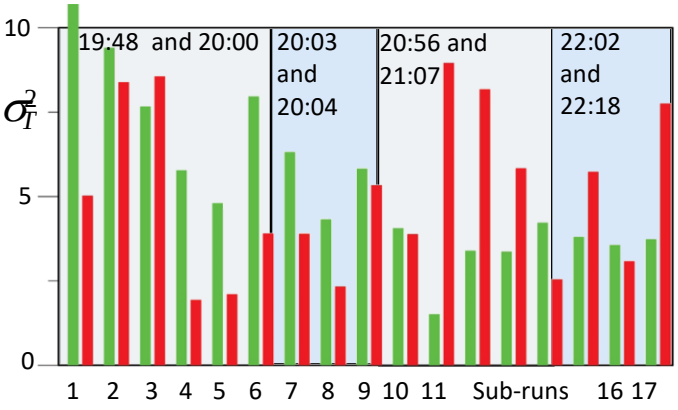

Comparison of temporal and spatial variances of intensity fluctuations

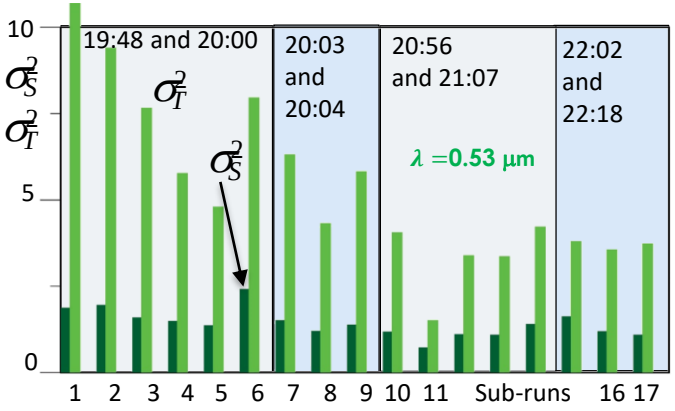

Variance of intensity fluctuations (1x1 mm pixel)

$$\sigma_N^2(\mathbf{r}_m)=\frac{\left\langle\left[I_n(\mathbf{r}_m)-\bar{I}_n(\mathbf{r}_m)\right]^2\right\rangle_N}{\bar{I}^2(\mathbf{r}_m)}$$

Averaged over aperture area variance of intensity fluctuations inside a pixel ("temporal" variance)

$$\sigma_T^2=\left\langle\sigma_N^2(\mathbf{r}_m)\right\rangle_{aperture}$$

Recording parameters

Number of frames for λ_1=0.53 μm	2850-2980
Number of frames for λ_2=1.06 μm	1170-1760
Duration of recording at both λ_1 and λ_2	30 sec

Experimental setup characteristic sizes

Aperture diameter	305 mm
Central obscuration diameter	102 mm
Pixel size	1mm x1 mm

Received Power-in-the-bucket (PIB) Fluctuations: Giant Spikes Observation

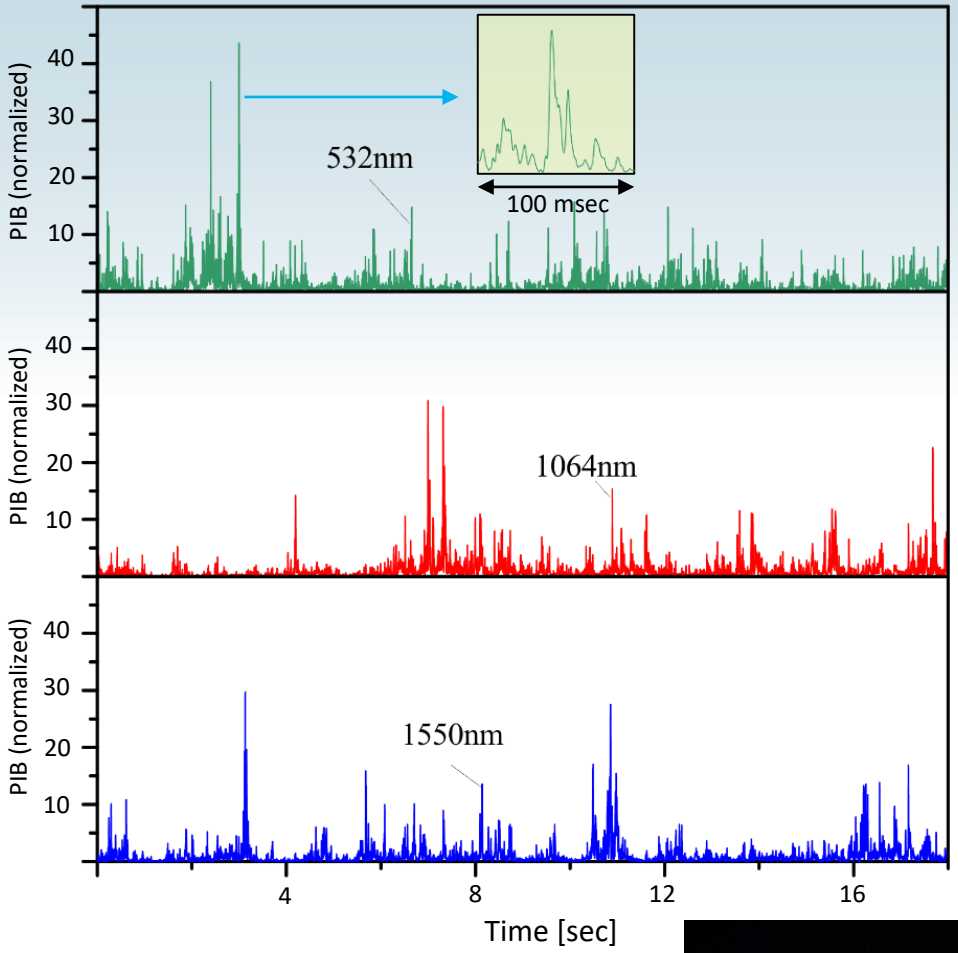

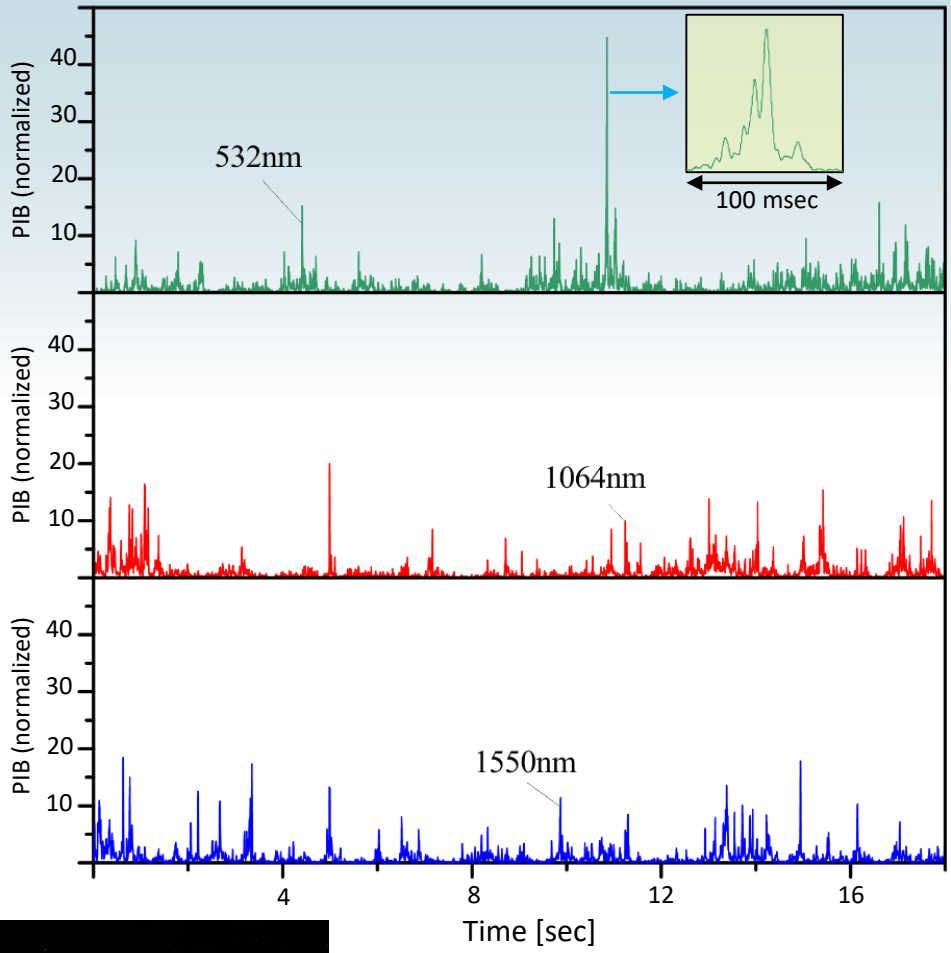

Date: April 5th; Local time: 20:40:20
Recording time 20s
Low-resolution vertical scan
Cn2 (MLO): 7.4e-15
Cn2 (HL): 7.1e-15

Date: April 5th , Local time: 20:29:20
Recording time 20s
Low-resolution vertical scan
Cn2 (MLO): 1.0e-14
Cn2 (HL): 4.5e-15

ERCAOS: Pupil Plane Scintillations (April 6)

λ=532 nm; 211 frames/sec

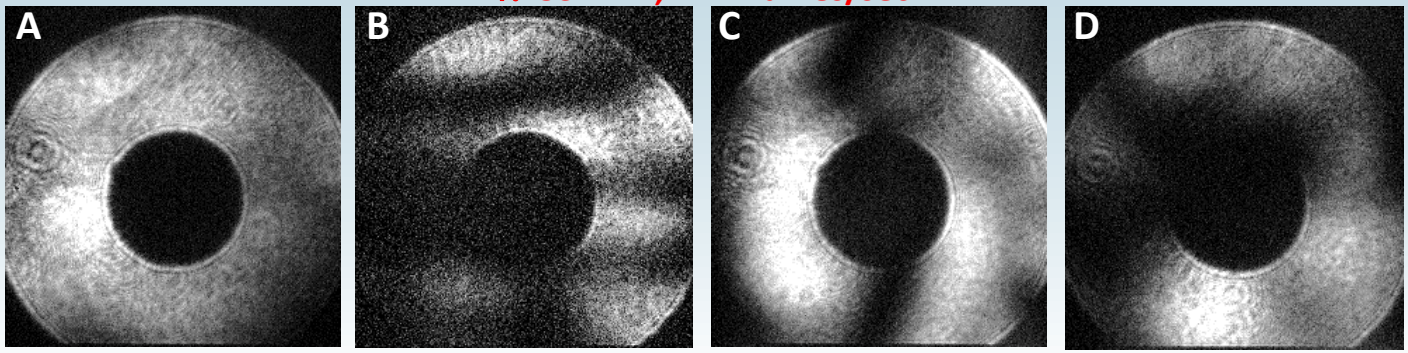

A: Integration time $1 \cdot 10^{-5}$ sec
recording at 21:54:55.92
frame #1040 at 21:55:06.22
B: Integration time $1 \cdot 10^{-5}$ sec
recording at 22:22:00.87
frame #1347 at 22:22:14.21
C: Integration time $1 \cdot 10^{-5}$ sec
recording at 22:41:29.50
frame #832 at 22:41:37.74
D: Integration time $1 \cdot 10^{-5}$ sec
recording at 23:10:09.10
frame #191 at 23:10:10.99

λ=1064 nm; 59 frames/sec

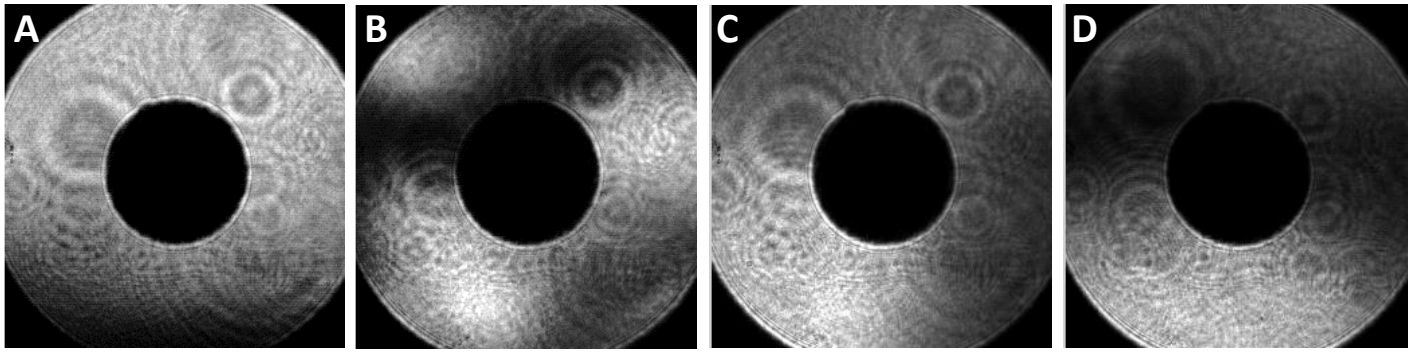

A: Integration time $2 \cdot 10^{-3}$ sec
recording at 21:54:55.92
frame #607 at 21:55:06.21
B: Integration time $2 \cdot 10^{-3}$ sec
recording at 22:22:35.05
frame #196 at 22:22:38.38
C: Integration time $2 \cdot 10^{-3}$ sec
recording at 22:42:03.71
frame #1321 at 22:42:15.05
D: Integration time $2 \cdot 10^{-3}$ sec
recording at 23:10:43.34
frame #109 at 23:10:45.19

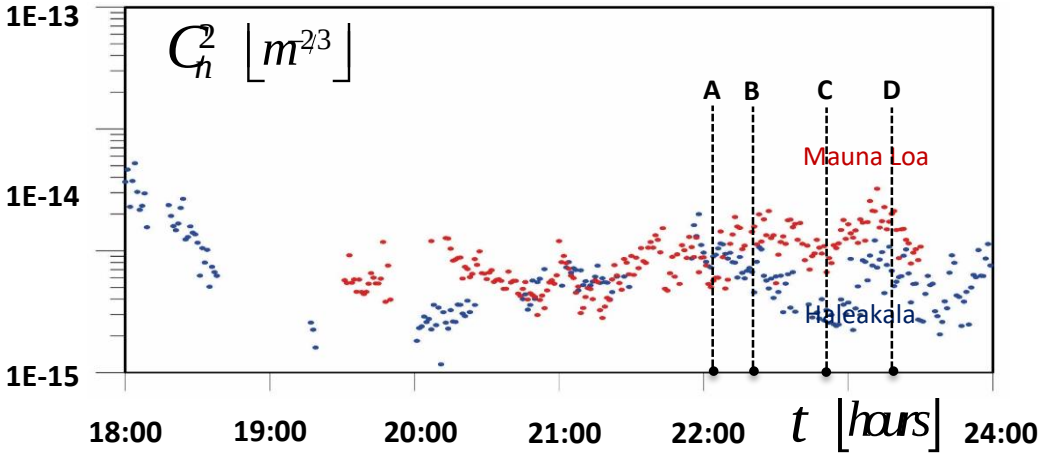

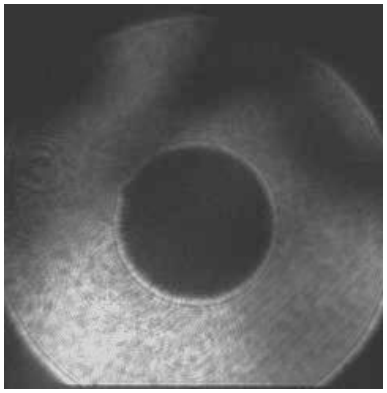

λ=532 nm

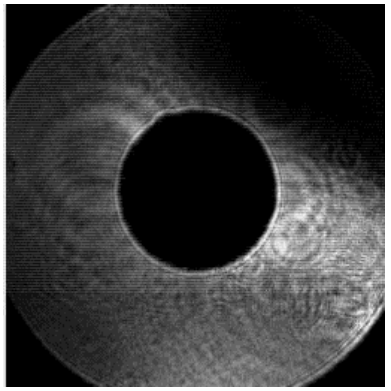

λ=1064 nm

ERCAOS: Pupil Plane Scintillations (April 14)

λ=532 nm; 211 frames/sec

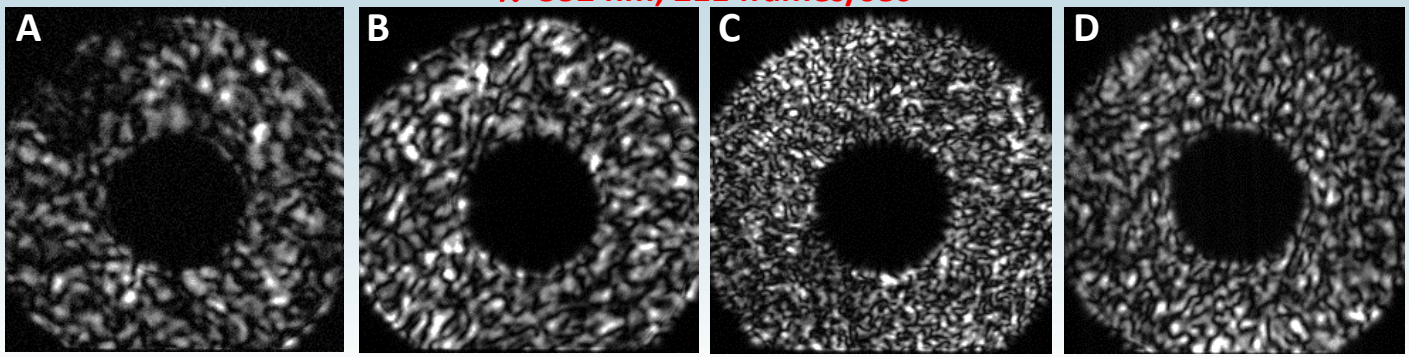

A: Integration time $6 \cdot 10^{-6}$ sec
recording at 20:52:11.97
frame #78 at 20:52:12.35
B: Integration time $2.3 \cdot 10^{-5}$ sec
recording at 21:23:59.50
frame #6114 at 21:24:28.47
C: Integration time $2.3 \cdot 10^{-5}$ sec
recording at 22:06:11.83
frame #246 at 22:06:12.99
D: Integration time $2.3 \cdot 10^{-5}$ sec
recording at 22:53:39.13
frame #557 at 22:53:41.77

λ=1064 nm; 59 frames/sec

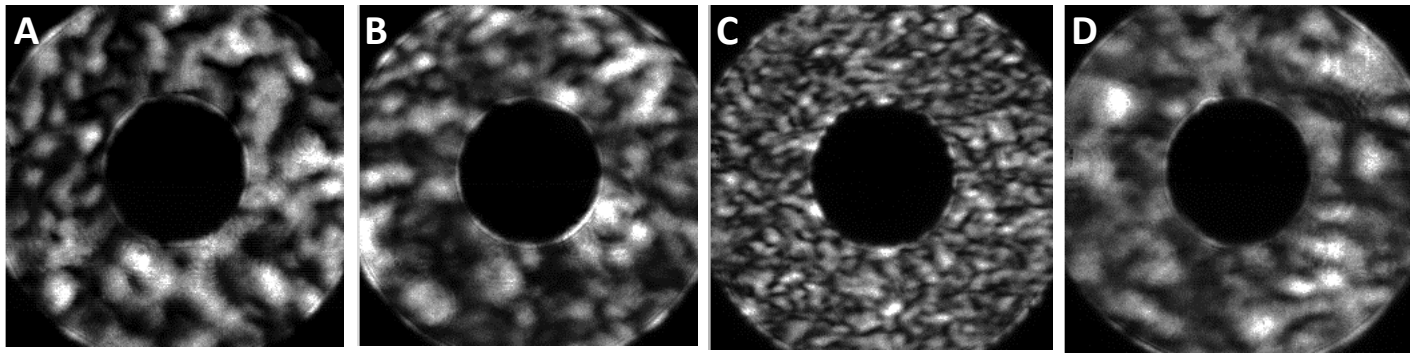

A: Integration time $1 \cdot 10^{-3}$ sec
recording at 20:53:03.25
frame #84 at 20:53:04.67
B: Integration time $1 \cdot 10^{-3}$ sec
recording at 21:24:50.72
frame #20 at 21:24:51.06
C: Integration time $1 \cdot 10^{-3}$ sec
recording at 22:07:03.03
frame #37 at 22:07:03.66
D: Integration time $1 \cdot 10^{-3}$ sec
recording at 22:54:30.18
frame #48 at 22:54:30.99

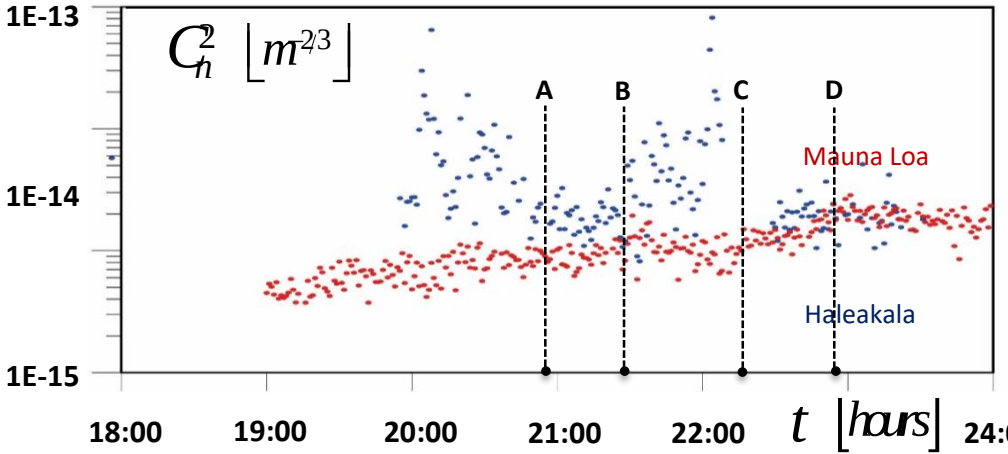

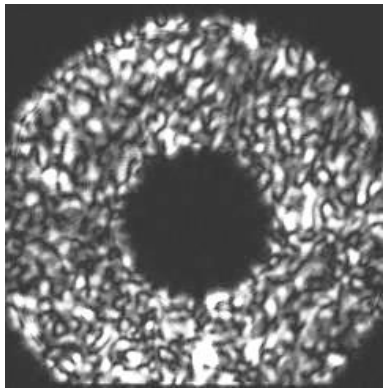

λ=532 nm

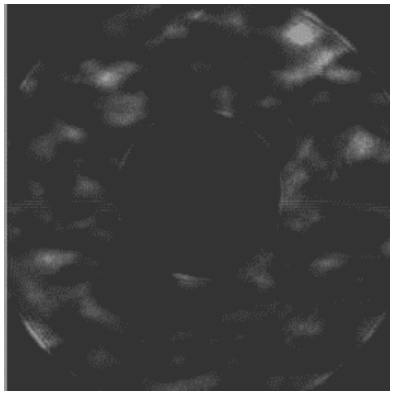

λ=1064 nm

Summary of Observed Intensity Scintillation Regimes

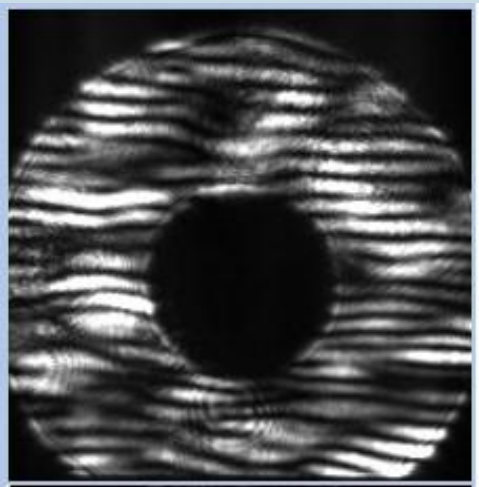
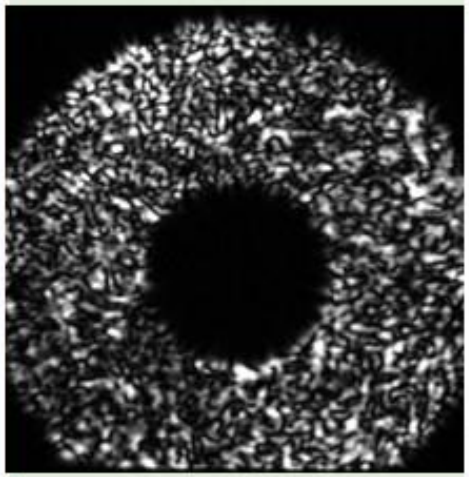
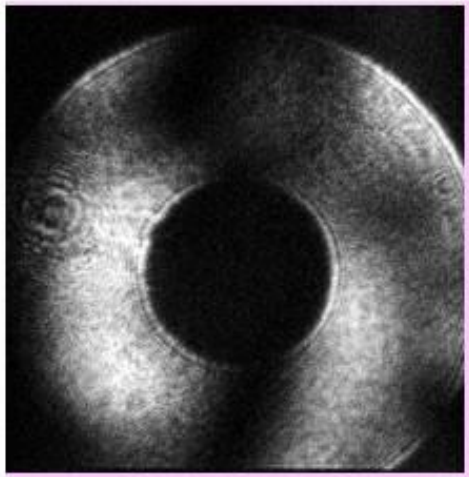
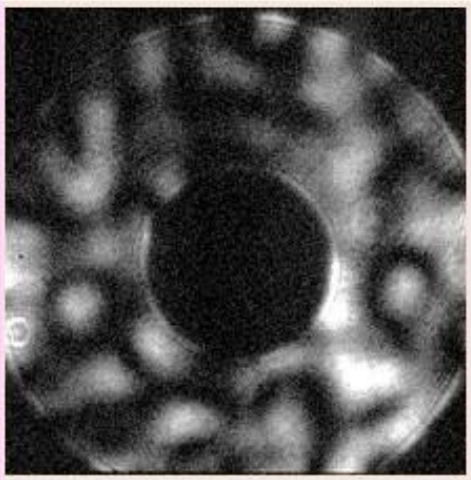
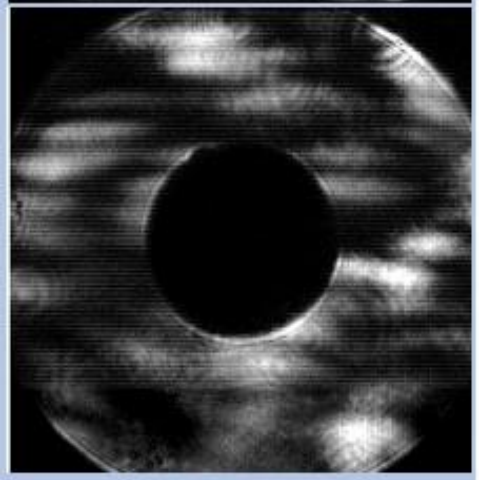
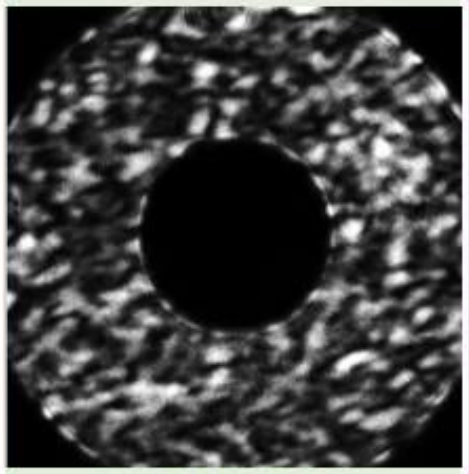
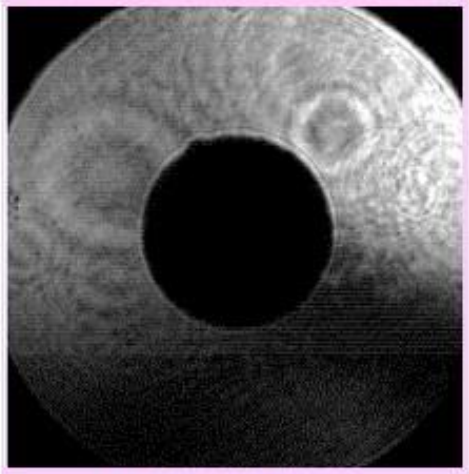
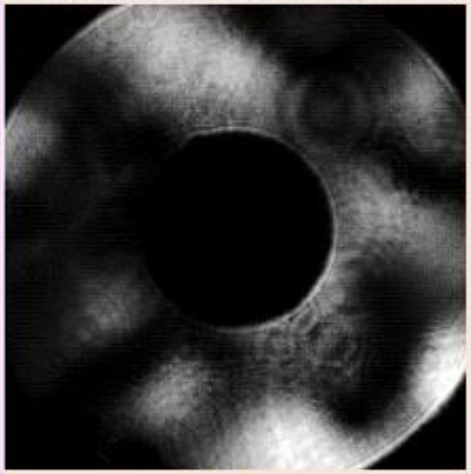

April 5, 2019
Mauna Loa
$C_n^2 = 1 \cdot 10^{-14}\ m^{-2/3}$
Haleakala
$C_n^2 = 5 \cdot 10^{-15}\ m^{-2/3}$

April 14, 2019
Mauna Loa
$C_n^2 = 1 \cdot 10^{-14}\ m^{-2/3}$
Haleakala
$C_n^2 = 5 \cdot 10^{-14}\ m^{-2/3}$

April 6, 2019
Mauna Loa
$C_n^2 = 1 \cdot 10^{-14}\ m^{-2/3}$
Haleakala
$C_n^2 = 3 \cdot 10^{-15}\ m^{-2/3}$

April 4, 2019
Mauna Loa
$C_n^2 = 8 \cdot 10^{-15}\ m^{-2/3}$
Haleakala
$C_n^2 = 3 \cdot 10^{-15}\ m^{-2/3}$

Beam Footprint & Refractivity-Induced Centroid Displacement Estimation

PIB profiles obtained with 1-D polychromatic beam vertical scanning (averaged over 20 scans)

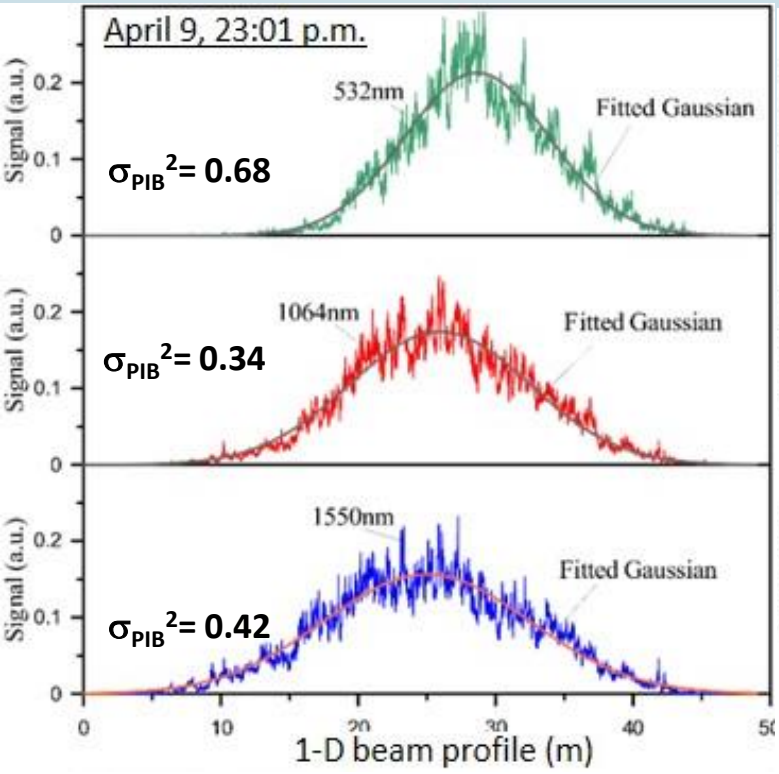

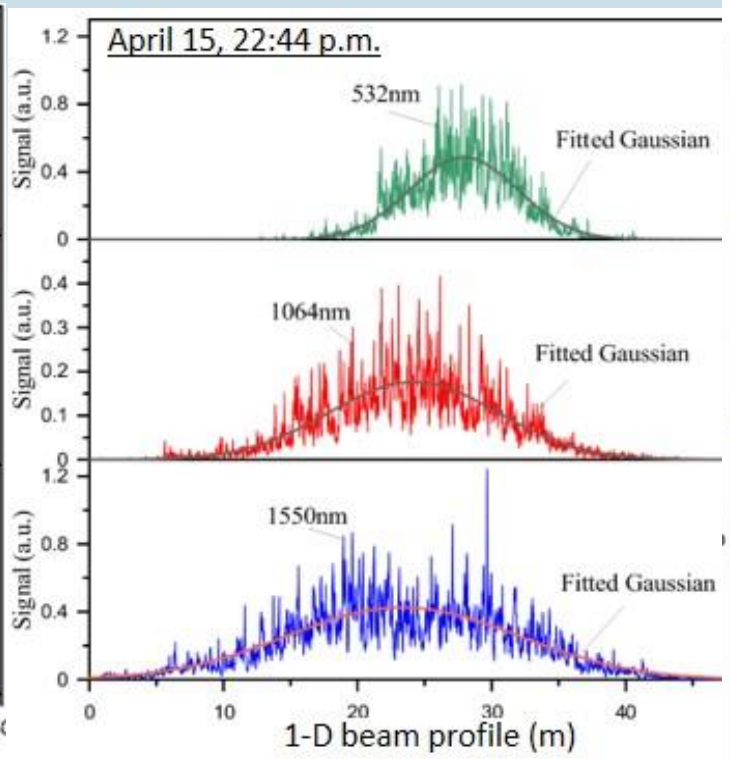

Images of polychromatic beam 2-D scan (April 15,2019)

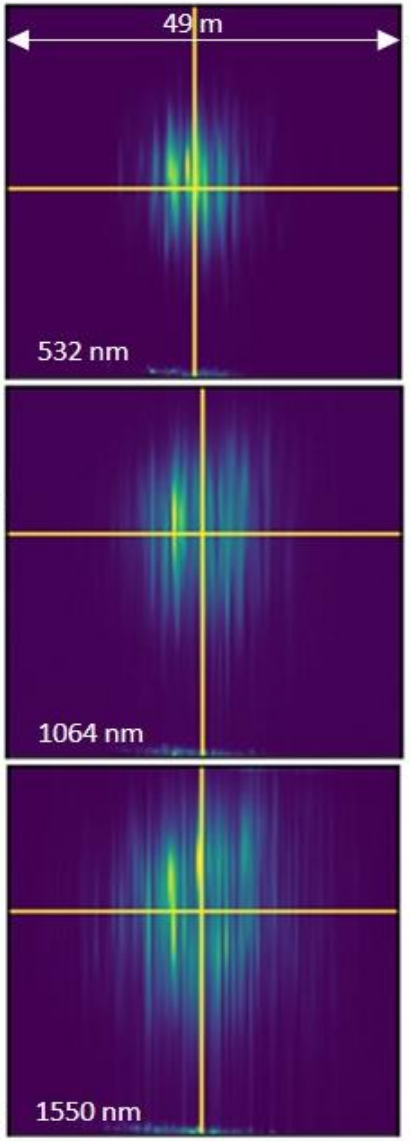

Date: April 9 Local time: 23:01

Mauna Loa $C_n^2 = 4 \cdot 10^{-15}\ m^{-2/3}$

Haleakala $C_n^2 = 5.2 \cdot 10^{-15}\ m^{-2/3}$

Exit-plane widths of transmitted beams	Beam footprint in vacuum
532 nm (12.0 mm / 12.4 mm)	532 nm 5.8 m
1064 nm (25 mm / 28 mm)	1064 nm 5.3 m
1550 nm (34 mm / 36 mm)	1550 nm 5.7 m

Vertical scan results

Beam footprint diameter (e^{-2} drop)	
532 nm	21 m
1064 nm	26.2 m
1550 nm	30.1 m

Beam footprint centroid shift	
532 -> 1064	2.71 m
532 ->1550	3.65 m

Refractivity-Induced Vertical Shift of Beam Centroids: Measurements vs Predictions Based on Standard Atmosphere (US1976) Model

Results of direct measurements of beam footprint centroid vertical displacements using polychromatic beam scanning technique: λ=1.55 μm relative to λ=0.53 μm (blue bars) & λ=1.06 μm relative to λ=0.53 μm (red bars)

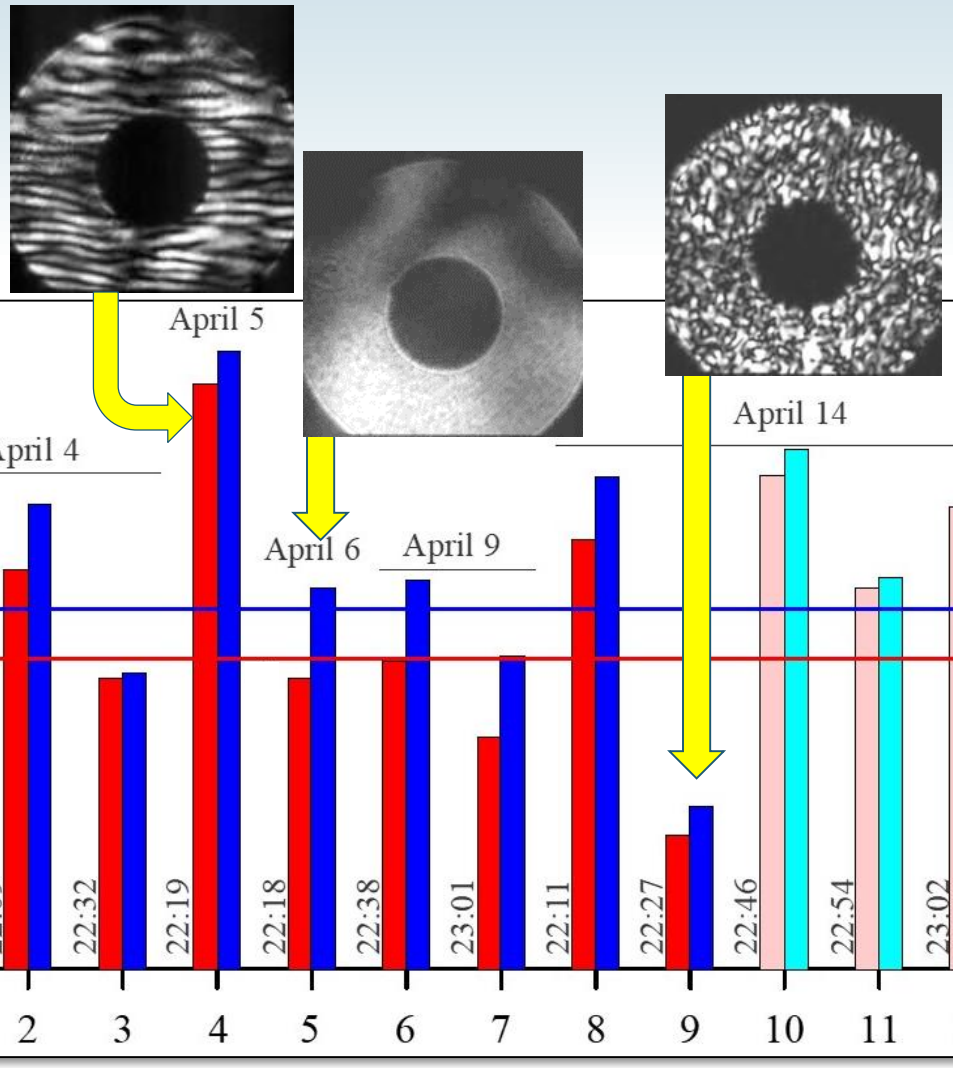

Summary of 149 km Laser Beam Propagation Experiments

- Observation of fringe-type pupil-plane laser beam intensity patterns and two well-defined focal spots at the receiver telescope - coherent laser beam “mirages”
- Observation of giant enhancement of turbulence strength and its impact on laser beam characteristics in the vicinity of clouds
- Observation of high variability of atmospheric refractivity and strong coupling of refractivity and turbulence-induced effects on laser beam propagation characteristics. Both, the observed vertical elongation of laser beam footprint, its size and centroid displacement magnitude were continuously changing during experiments within a characteristic time scale of a few minutes
- Observation and quantitative measurements of the horizontal and vertical anisotropy of laser beam widening over long range atmospheric propagation in presence of both turbulence and refractivity. These measurements were performed via transmitted polychromatic beam scanning with simultaneous measurements of the PIB signal by the polychromatic receiver
- Qualitative measurements of laser beam intensity scintillations and frequency of giant spikes appearance.
- Simultaneous recording of both meteorological and optical turbulence characteristics at both sides of the propagation path


THE END